Development of interharmonics identification using enhanced-FFT algorithm

Hsiung Cheng Lin

Department of Electronic Engineering, National Chin-Yi University of Technology, Taiwan
E-mail: hclin@ncut.edu.tw

Published in *The Journal of Engineering*; Received on 7th April 2017; Accepted on 9th June 2017

Abstract: The fast Fourier transform (FFT) is a mostly used tool to measure power system harmonics. FFT, however, is not applicable to analyse interharmonics due to spectral leakage effect. Although International Electrotechnical Commission (IEC) standard is recommended for interharmonic measurement, the individual interharmonic frequency and respective amplitude cannot be worked out under this framework. For this reason, this paper proposes an enhanced-FFT model to build up the relationship between interharmonic frequency and dispersed leakage energy. The mathematical equation is thus established to find actual value of interharmonic frequency. Moreover, the true interharmonic amplitude can be retrieved from the dispersed energy collection. In other words, the sampling window length is no longer required to match the interharmonic period and the correct measurement results can be achieved. The proposed model is developed using a simple arithmetic equation so that it is feasible for more efficient calculation for interharmonic analysis. Performance results verify that the proposed scheme can achieve accurate, rapid and reliable outcomes.

1 Introduction

With an increasing number of power electronics facilities used in industry, the power line pollution has been seriously deteriorated due to harmonics generated in electric power system. The situation even worsens when the applications of periodical time-varying apparatuses grow and produce interharmonics sequentially in recent years. It is well known that interharmonics frequencies are not an integer of the fundamental components, and it is thought as the inter-modulation between the fundamental and harmonic components in the system. Major sources have been found in cycloconverters, wind turbine, double conversion system, time-varying loads, variable-load electric drives and unexpected sources [1–3]. In addition to typical problems caused by harmonics, interharmonics bring new problems such as thermal effects, cathode ray tube flicker, saturation of current transformers, low-frequency oscillation in a mechanical system, voltage fluctuations, subsynchronous oscillation etc. Even under low amplitude of interharmonic, the above phenomena may still exist [4–6].

Although FFT is still the most popular method in harmonics analysis, incorrect results may arise if the sampling window length is not properly chosen. When the measured waveforms contain interharmonics, FFT will suffer from low accuracy and less computational efficiency [7–9]. For this reason, an adaptive window width approach was announced to estimate harmonics/interharmonics [10]. However, a large initial value is required for the generic waveform to avoid deceptively strong correlation. A long computational time during the iteration process is therefore needed. Another way that combined Prony-based and downsampling techniques was reported for harmonics and interharmonics measurement [11]. Unfortunately, the selection of the downsampling coefficient and estimation order is difficult to be formulated because of sensitivity to the measured signal. The exact model order ESPRIT algorithm based on the RD plot is another approach that improved the sliding-window ESPRIT method; however, its computational time was a big concern in practice [12]. An interpolated discrete Fourier transform (DFT) can reduce the spectral leakage and thus find the correct parameter values of signals [13]. The measurement accuracy, however, may be influenced by the location of the interharmonic frequency component. The sliding-window ESPRIT algorithm was proposed for the frequency estimation of interharmonics [14]. In this model, the interharmonic number is required prior to implementation, and it may lead to spurious components, line splitting and occasional failure. Recently, a new approach using single channel independent component analysis for both harmonics and interharmonics was reported. The orthogonal vector of the proposed model may be unconvinced in convergence [15]. Recently, a group-harmonic power minimising algorithm for harmonics and interharmonics estimation was reported [16]. Although this method can achieve an accurate measurement, a searching procedure was required to reach the solution. Some studies have applied neural network models to carry out both harmonic/interharmonic analysis [17–19]. However, their initial parameter settings usually rely on trial and error. This is somehow discouraged in a real application.

Indeed, the presence of interharmonics poses measurement more difficulties for some reasons: (i) very low values of interests of interharmonics (about one order of quantity smaller than harmonics); (ii) variability of frequency, and amplitude; (iii) variability of the waveform periodicity; (iv) great sensitivity to the spectral leakage phenomenon. To address aforementioned issues, a guideline for interharmonics measurement based on grouping concept was suggested by IEC 61000-4-7 standard [20]. A 5 Hz frequency resolution with rectangular window is recommended to be adopted; however, individual interharmonic information is unavailable from such a measurement.

2 Enhanced-FFT (e-FFT) model

2.1 Background of Fourier transformation

A periodical waveform can be reconstructed by series harmonic components via the Fourier transform (FT) analysis, where harmonic frequency is defined as a multiple of fundamental. Assume a waveform $i_s(t)$ is periodical with satisfaction of Dirichlet condition, it can be expressed as

$$i_s(t) = \sum_{n=-\infty}^{\infty} i_n e^{j2\pi nft} \tag{1}$$

where $i_n = (1/T)\int_0^T i_s(t)e^{-j2\pi nft}\,dt$, and $T(=1/f)$ is the signal period. i_0 is the dc component.

For performing FT, DFT is then introduced as

$$i_s[n] = \sum_{k=0}^{N-1} I_s[k]W_N^{kn} \tag{2}$$

where $I_s[k] = (1/N)\sum_{n=0}^{N-1} i_s[n]W_N^{-kn}$, and $W_N = \exp(j2\pi/N)$.

doi: 10.1049/joe.2017.0133

The Fourier fundamental angular frequency ($\Delta\omega$) for $i_s[n]$ with the period T is defined as

$$\Delta\omega = \frac{2\pi}{T} \tag{3}$$

When the waveform is sampled using $p(p>1)$ periods, $\Delta\omega$ can be represented as

$$\Delta\omega = \frac{2\pi}{pT} = \frac{\omega_0}{p} \tag{4}$$

where $\omega_0 = 2\pi/T$.

From (4), the Fourier fundamental frequency (Δf) is defined as

$$\Delta f = \frac{1}{pT} = \frac{1}{pN_sT_s} = \frac{1}{NT_s} = \frac{f_s}{N} \tag{5}$$

where $N_s \triangleq N/p$, and $T_s \triangleq 1/f_s$. It is noted that N points is sampled using the sampling rate f_s.

The waveform power (P) can be expressed by the Parseval relation as [21, 22]

$$P = \frac{1}{N}\sum_{n=0}^{N-1} i_s[n]^2 = \sum_{k=0}^{N-1} I_s[k]^2 \tag{6}$$

The power at the frequency f_k can be expressed as

$$P[f_k] = I_s[k]^2 + I_s[N-k]^2 = 2I_s[k]^2 \tag{7}$$

where $k = 0, 1, 2,\ldots,N/2-1$.

The amplitude of the mth harmonic at f_k is then calculated as

$$A_m[f_k] = \sqrt{P[f_k]} = \sqrt{2}I_s[k] \tag{8}$$

where $m = 1, 2,\ldots,M$.

It is known that interharmonics contained in a waveform is not synchronised with the fundamental. As a result, the mth harmonic power at f_k disperses over around the f_k. Based on the concept of group harmonics, all spilled power around the adjacent harmonics can be collected into a 'group power' as [20]

$$P_m^*[f_k] = \sum_{\Delta k=-\tau}^{+\tau} (A_m[f_{k+\Delta k}])^2 \tag{9}$$

where τ denotes the group bandwidth.

As above, the true harmonic amplitude can be retrieved from collection of all dispersed power as

$$A_m^*[f_k] = \sqrt{P_m^*[f_k]} \tag{10}$$

2.2 e-FFT algorithm

The proposed e-FFT model is based on the FFT for suiting interharmonics measurement. According to the FFT analysis, the relationship between harmonic frequency and dispersed energy can be classified into two cases: small and big frequency deviation [23]. Case 1: Depiction for small frequency deviation is shown in Fig. 1*a*, where the second larger magnitude ($A_m[f_{k+1}]$) at f_{k+1} is located at the right side of the dominant frequency at f_k with $A_m[f_k] > A_m[f_{k+1}]$. In view of practice, however, f_k may be wrongly interpreted as the dominant harmonic. The situation is that the true frequency is equal to f_k plus the 'frequency deviation' (Δf_k) defined in (11). On the other hand, it reveals that higher $A_m[f_{k+1}]$ introduces more amount of deviation (Δf_k) distant from f_k. Case 2: Depiction for a big frequency deviation is shown in Fig. 1*b*, where the second larger amplitude ($A_m[f_k]$) at f_k is located at the left-hand side of the dominant frequency at f_{k+1} with $A_m[f_k] < A_m[f_{k+1}]$. The f_{k+1} may be wrongly interpreted as the dominant harmonic frequency in this case. Indeed, the true

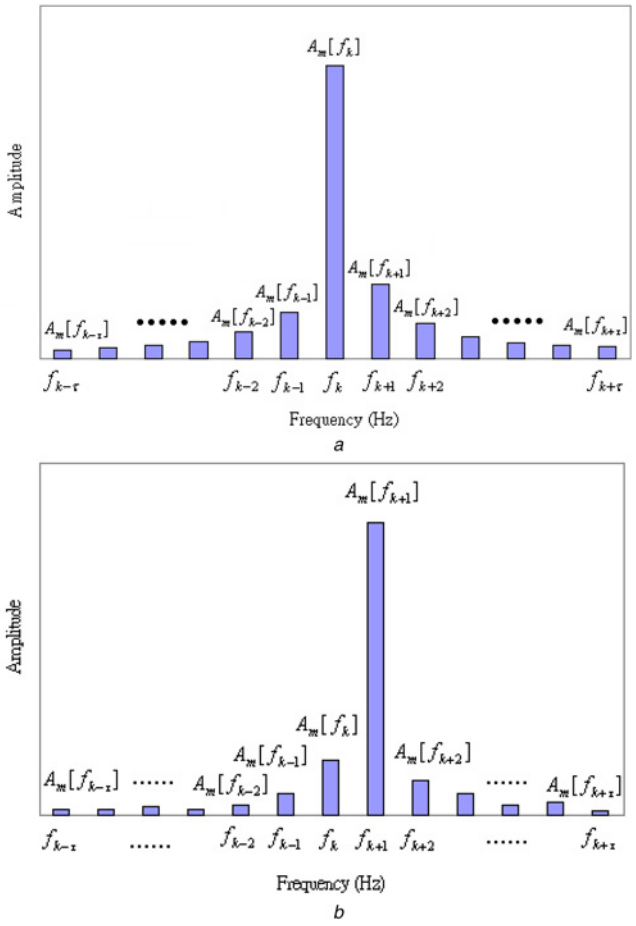

Fig. 1 *Relation between harmonic frequency and dispersed energy [23]*
a Small frequency deviation
b Big frequency deviation

frequency should be equal to f_k plus the 'frequency deviation' (Δf_k). Higher $A_m[f_{k+1}]$ also introduces more amount of deviation (Δf_k) distant from f_k. As illustrated above, both small and big frequency deviation are defined based on the generic phenomenon of frequency deviation condition, where 'small' and 'big' only denotes the deviation status rather than a real value.

The e-FFT model is formulated from the relation between the frequency deviation amount and dispersed energy distribution [6]. It is induced that the real frequency can be represented by the dominant frequency (f_k) plus 'frequency deviation' (Δf_k), i.e. $f_k + \Delta f_k$.

The frequency deviation range (FDR) is defined as

$$\Delta f_k = \frac{\sqrt{\sum_{\Delta k=1}^{+\tau} A_m[f_{k+\Delta k}]^2}}{\sqrt{\sum_{\Delta k=-\tau}^{0} A_m[f_{k+\Delta k}]^2} + \sqrt{\sum_{\Delta k=1}^{+\tau} A_m[f_{k+\Delta k}]^2}} \cdot \Delta f \tag{11}$$

where Δf is determined by N and f_s due to $\Delta f = f_s/N$, and $\tau = 0, 1, 2, 3, \ldots$.

From the group-harmonic concept, the dispersed energy around the major harmonic can be efficiently collected for retrieving the original amplitude [20]. Thus, the Restored Amplitude (RA) can be defined as

$$\text{R.A.} = \sqrt{\sum_{\Delta k=-\tau}^{+\tau} A_m[f_{k+\Delta k}]^2} \tag{12}$$

where $\tau = 0, 1, 2, 3, \ldots$.

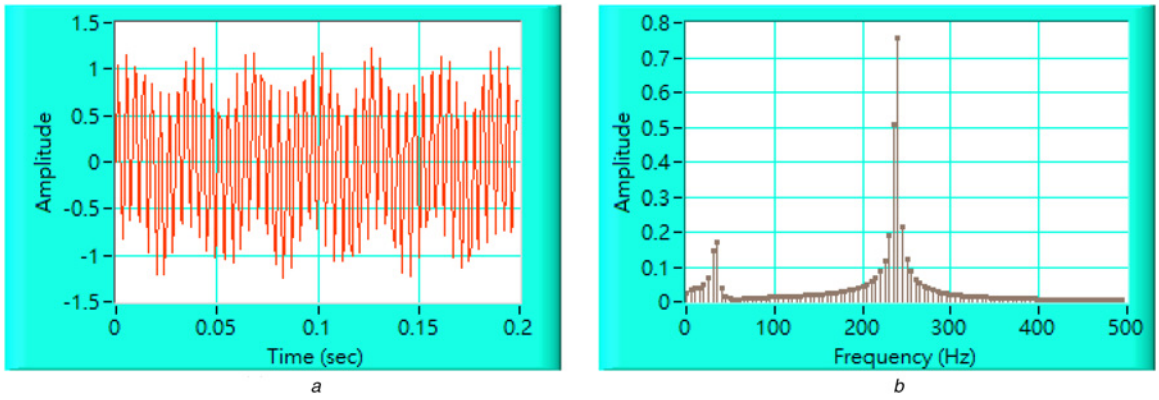

Fig. 2 *Spectrum of v(t) using FFT*
a Waveform
b Spectrum

The following example is used to demonstrate the calculation of Δf and RA. Assume the signal, i.e. $i(t) = 0.25\sin(2\pi \cdot 33 \cdot t) + 1.0\sin(2\pi \cdot 238 \cdot t)$, contains two major harmonics located at 33 and 238 Hz, and their amplitudes are set as 0.3 and 1.0, respectively. Please note that $f_s = 1.28$ kHz, $N = 256$ and $\tau = 5$, where $\Delta f = 5$ Hz. The waveform and its spectrum using FFT are shown in Figs. 2*a* and *b*, respectively. At both 33 and 238 Hz, it can be seen that some energy are dispersed around the neighbour sides considerably.

At 33 Hz, the FDR beyond 30 Hz can be calculated using (11) as

(see equations (13) and (14))

This interharmonic frequency (33 Hz) is found equal to 30 Hz (f_k) plus 2.5 Hz (Δf_k), close to the actual frequency value (33 Hz). Its RA is 0.24 that is close to the actual amplitude value (0.25).

At 238 Hz, the FDR beyond 235 Hz can be calculated using (11) as

(see equations (15) and (16))

This interharmonic frequency (238 Hz) is found equal to 235 Hz (f_k) plus 2.9 Hz (Δf_k), very close to the actual frequency value (238 Hz). Its RA is 0.98 that is very close to the actual amplitude value (1.0).

The τ is set as five for the above case. In reality, the selection of group bandwidth ($\tau = 1$–5) should consider harmonics locations to avoid overlapping between each other. Based on this principle, the e-FFT model is formulated by the following rule:

$$
\begin{aligned}
&|f_1 - f_2| < 4\Delta f \Rightarrow \tau = 1\\
&4\Delta f \le |f_1 - f_2| < 6\Delta f \Rightarrow \tau = 2\\
&6\Delta f \le |f_1 - f_2| < 8\Delta f \Rightarrow \tau = 3\\
&8\Delta f \le |f_1 - f_2| < 10\Delta f \Rightarrow \tau = 4\\
&|f_1 - f_2| \ge 10\Delta f \Rightarrow \tau = 5
\end{aligned}
$$

where f_1 and f_2 are assumed as two arbitrary near major harmonics in the waveform.

The flowchart of the proposed e-FFT model is shown in Fig. 3, and its performance procedure is demonstrated as follows [24].

(i) Select f_s, N and sample the signal.
(ii) Perform FFT.
(iii) Determine the number (M) of major harmonics.
(iv) Define the biggest amplitude and second big amplitude at f_1 and f_2, respectively.
(v) Check if $|f_1 - f_2| < 4\Delta f$. If yes, select $\tau = 1$ and go to Step 10. Otherwise, go to next step.

$$
\begin{aligned}
\Delta f_k &= \frac{\sqrt{0.17^2 + 0.037^2 + 0.015^2 + 0.0078^2 + 0.0057^2}}{\sqrt{0.037^2 + 0.041^2 + 0.048^2 + 0.066^2 + 0.14^2} + \sqrt{0.17^2 + 0.037^2 + 0.015^2 + 0.0078^2 + 0.0057^2}} \cdot \Delta f \\
&= \frac{0.175}{0.175 + 0.175} \cdot 5 \simeq 2.5\,(\text{Hz})
\end{aligned} \tag{13}
$$

$$
\begin{aligned}
\text{R.A.} &= \sqrt{0.037^2 + 0.041^2 + 0.048^2 + 0.066^2 + 0.14^2 + 0.17^2 + 0.037^2 + 0.015^2 + 0.0078^2 + 0.0057^2} \\
&\simeq 0.24
\end{aligned} \tag{14}
$$

$$
\begin{aligned}
\Delta f_k &= \frac{\sqrt{0.75^2 + 0.21^2 + 0.12^2 + 0.086^2 + 0.066^2}}{\sqrt{0.069^2 + 0.087^2 + 0.12^2 + 0.19^2 + 0.51^2} + \sqrt{0.75^2 + 0.21^2 + 0.12^2 + 0.086^2 + 0.066^2}} \cdot \Delta f \\
&= \frac{0.8}{0.57 + 0.8} \cdot 5 \simeq 2.9\,(\text{Hz})
\end{aligned} \tag{15}
$$

$$
\begin{aligned}
\text{R.A.} &= \sqrt{0.069^2 + 0.087^2 + 0.12^2 + 0.19^2 + 0.51^2 + 0.75^2 + 0.21^2 + 0.12^2 + 0.086^2 + 0.066^2} \\
&\simeq 0.98 \cong 1.0
\end{aligned} \tag{16}
$$

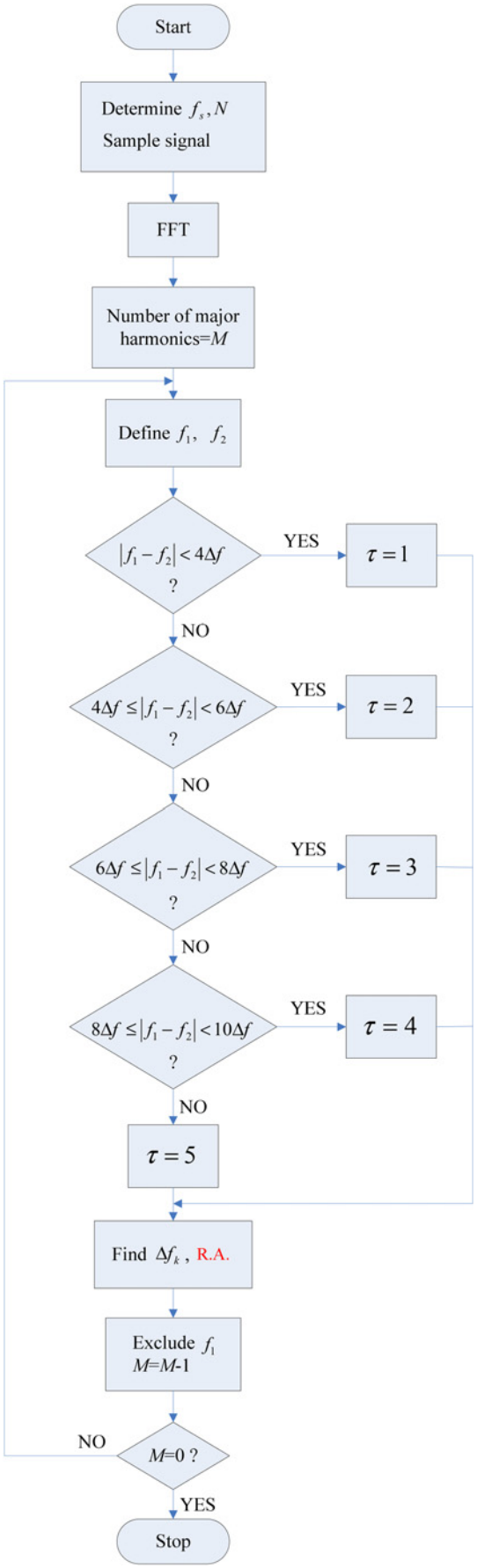

Fig. 3 *Flowchart of the proposed e-FFT model*

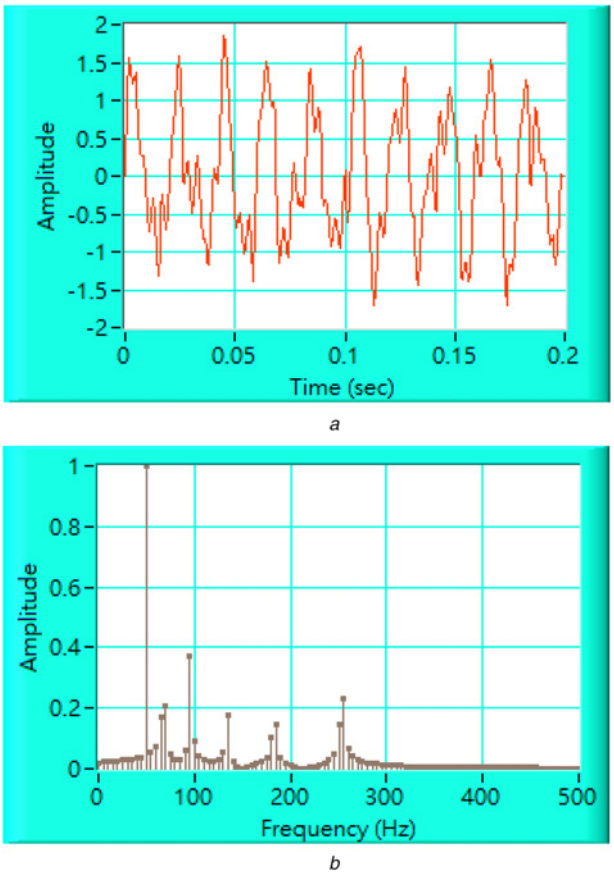

Fig. 4 *Analysis of $s(t)$ with $\Delta f = 5$ Hz*
a Waveform of $s(t)$
b Spectrum of $s(t)$ using FFT

(vi) Check if $4\Delta f \le |f_1 - f_2| < 6\Delta f$. If yes, select $\tau = 2$ and go to Step 10. Otherwise, go to next step.
(vii) Check if $6\Delta f \le |f_1 - f_2| < 8\Delta f$. If yes, select $\tau = 3$ and go to Step 10. Otherwise, go to next step.
(viii) Check if $8\Delta f \le |f_1 - f_2| < 10\Delta f$. If yes, select $\tau = 4$ and go to Step 10. Otherwise, go to next step.
(ix) Select $\tau = 5$.
(x) Calculate Δf_k, RA
(xi) Exclude the f_1 component (the biggest amplitude) that has been identified, and $M = M - 1$.
(xii) Check if $M = 0$. If yes, the procedure stops. Otherwise, go back to Step 4.

3 Model verification

3.1 Model performance

To verify the proposed model, the waveform $s(t)$ is tested.

$$s(t) = a_1 \sin(2\pi \cdot f_1 \cdot t) + a_{i1} \sin(2\pi \cdot f_{i1} \cdot t) + a_{i2} \sin(2\pi \cdot f_{i2} \cdot t) + a_{i3} \sin(2\pi \cdot f_{i3} \cdot t) + a_{i4} \sin(2\pi \cdot f_{i4} \cdot t) + a_{i5} \sin(2\pi \cdot f_{i5} \cdot t) \quad (17)$$

where $a_1 = 1.0$ is the amplitude of the fundamental, and its respective frequency is $f_1 = 50$ Hz. The amplitudes of interharmonics are $a_{i1} = 0.3$, $a_{i2} = 0.4$, $a_{i3} = 0.2$, $a_{i4} = 0.2$, $a_{i5} = 0.3$, and their respective frequencies are $f_{i1} = 68$ Hz, $f_{i2} = 96$ Hz, $f_{i3} = 134$ Hz, $f_{i4} = 183$ Hz, $f_{i5} = 253$ Hz.

The waveform of $s(t)$ shown in Fig. 4*a*, and its spectrum using FFT is shown in Fig. 4*b*. It is obvious that a considerable dispersed power always comes with interharmonics and thus causes incorrect results.

3.1.1 Analysis with Δf = 5 Hz: The parameters of e-FFT model are set as $f_s = 1.28$ kHz, $N = 256$, i.e. $\Delta f = 5$ Hz. The interharmonics analysis using e-FFT model is carried out by the following five cases from (17). According to the rule of group bandwidth (τ) selection, τ is chosen as follows:

(i) For $f_{i1} = 68$ Hz, $|f_{i1} - f_1| = |68 - 50| < 4\Delta f(=20) \Rightarrow \tau = 1$
(ii) For $f_{i2} = 96$ Hz, $4\Delta f(=20) \le |f_{i2} - f_{i1}| = |96 - 68| < 6\Delta f(=30) \Rightarrow \tau = 2$
(iii) For $f_{i3} = 134$ Hz, $6\Delta f(=30) \le |f_{i3} - f_{i2}| = |134 - 96| < 8\Delta f(=40) \Rightarrow \tau = 3$
(iv) For $f_{i4} = 183$ Hz, $8\Delta f(=40) \le |f_{i4} - f_{i3}| = |183 - 134| < 10\Delta f(=50) \Rightarrow \tau = 4$
(v) For $f_{i5} = 253$ Hz, $|f_{i5} - f_{i4}|(=253 - 183) \ge 10\Delta f(=50) \Rightarrow \tau = 5$

Consequently,
Case 1: $a_{i1} = 0.3, f_{i1} = 68$ Hz, $\tau = 1$

$$\Delta f_k = \frac{\sqrt{0.21^2}}{\sqrt{0.075^2 + 0.17^2} + \sqrt{0.21^2}} \cdot \Delta f = \frac{0.21}{0.186 + 0.21} \cdot 5 \simeq 2.7\ (\text{Hz}) \tag{18}$$

$$\text{R.A.} = \sqrt{0.075^2 + 0.17^2 + 0.21^2} \simeq 0.28 \tag{19}$$

The measured frequency is equal to $f_k = 65$ Hz plus $\Delta f_k = 2.7$ Hz, i.e. 67.7 Hz, very close to the real one (68 Hz). On the other hand, the measured amplitude is ∼0.28 that is also close to the real one (0.3).

Case 2: $a_{i2} = 0.4, f_{i2} = 96$ Hz, $\tau = 2$

$$\Delta f_k = \frac{\sqrt{0.093^2 + 0.041^2}}{\sqrt{0.061^2 + 0.37^2} + \sqrt{0.093^2 + 0.041^2}} \cdot \Delta f = \frac{0.10}{0.38 + 0.10} \cdot 5 \simeq 1.0\ (\text{Hz}) \tag{20}$$

$$\text{R.A.} = \sqrt{0.061^2 + 0.37^2 + 0.093^2 + 0.041^2} \simeq 0.39 \tag{21}$$

The measured frequency is equal to $f_k = 95$ Hz plus $\Delta f_k = 1.0$ Hz, i.e. 96 Hz, same as the real one (96 Hz). The measured amplitude is ∼0.39 that is very close to the real one (0.4).

Case 3: $a_{i3} = 0.2, f_{i3} = 134$ Hz, $\tau = 3$

$$\Delta f_k = \frac{\sqrt{0.18^2 + 0.022^2 + 0.0068^2}}{\sqrt{0.023^2 + 0.029^2 + 0.055^2} + \sqrt{0.18^2 + 0.022^2 + 0.0068^2}} \cdot \Delta f = \frac{0.18}{0.066 + 0.18} \cdot 5 \simeq 3.66\ (\text{Hz}) \tag{22}$$

$$\text{R.A.} = \sqrt{0.023^2 + 0.029^2 + 0.055^2 + 0.18^2 + 0.022^2 + 0.0068^2} \simeq 0.19 \tag{23}$$

It is found that the measured frequency is equal to $f_k = 130$ Hz plus $\Delta f_k = 3.66$ Hz, i.e. 133.66 Hz, almost same as the real one (134 Hz). The measured amplitude is ∼0.19 that is very close to the real one (0.2).

Case 4: $a_{i4} = 0.2, f_{i4} = 183$ Hz, $\tau = 4$

(see equations (24) and (25))

The above results indicate that the measured frequency is equal to $f_k = 180$ Hz plus $\Delta f_k = 2.87$ Hz, i.e. 182.87 Hz, almost same as the real one (183 Hz). The measured amplitude is ∼0.19 that is very close to the real one (0.2).

Case 5: $a_{i5} = 0.3, f_{i5} = 253$ Hz, $\tau = 5$

(see equations (26) and (27))

As above, the measured frequency is equal to $f_k = 180$ Hz plus $\Delta f_k = 2.87$ Hz, i.e. 182.87 Hz, almost same as the real one (183 Hz). The measured amplitude is ∼0.19 that is very close to the real one (0.2).

The measured spectrum using e-FFT is shown in Fig. 5, indicating no dispersed power around harmonics/interharmonics.

The comparison between FFT and e-FFT is concluded in Fig. 6. As can be seen, the results from e-FFT model are almost identical to the real values for either amplitude or frequency identification, but traditional FFT is unable to achieve a correct analysis except at fundamental component (50 Hz). The maximum error for amplitude and frequency estimation using FFT is up to 30 and 4.41%, respectively. By contrast, the maximum error for amplitude and frequency estimation using e-FFT is only 6.67 and 0.44%, respectively.

$$\Delta f_k = \frac{\sqrt{0.15^2 + 0.039^2 + 0.02^2 + 0.012^2}}{\sqrt{0.015^2 + 0.023^2 + 0.039^2 + 0.1^2} + \sqrt{0.15^2 + 0.039^2 + 0.02^2 + 0.012^2}} \cdot \Delta f = \frac{0.155}{0.115 + 0.155} \cdot 5 \simeq 2.87\ (\text{Hz}) \tag{24}$$

$$\text{R.A.} = \sqrt{0.015^2 + 0.023^2 + 0.039^2 + 0.1^2 + 0.15^2 + 0.039^2 + 0.02^2 + 0.012^2} \simeq 0.19 \tag{25}$$

$$\Delta f_k = \frac{\sqrt{0.23^2 + 0.07^2 + 0.042^2 + 0.031^2 + 0.024^2}}{\sqrt{0.012^2 + 0.018^2 + 0.028^2 + 0.051^2 + 0.15^2} + \sqrt{0.23^2 + 0.07^2 + 0.042^2 + 0.031^2 + 0.024^2}} \cdot \Delta f = \frac{0.249}{0.158 + 0.249} \cdot 5 \simeq 3.06\ (\text{Hz}) \tag{26}$$

$$\text{R.A.} = \sqrt{0.012^2 + 0.018^2 + 0.028^2 + 0.051^2 + 0.15^2 + 0.23^2 + 0.07^2 + 0.042^2 + 0.031^2 + 0.024^2} \simeq 0.3 \tag{27}$$

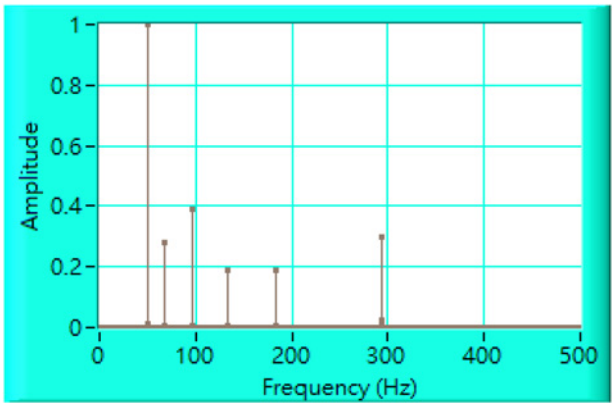

Fig. 5 *Spectrum of s(t) using e-FFT with Δf = 5 Hz*

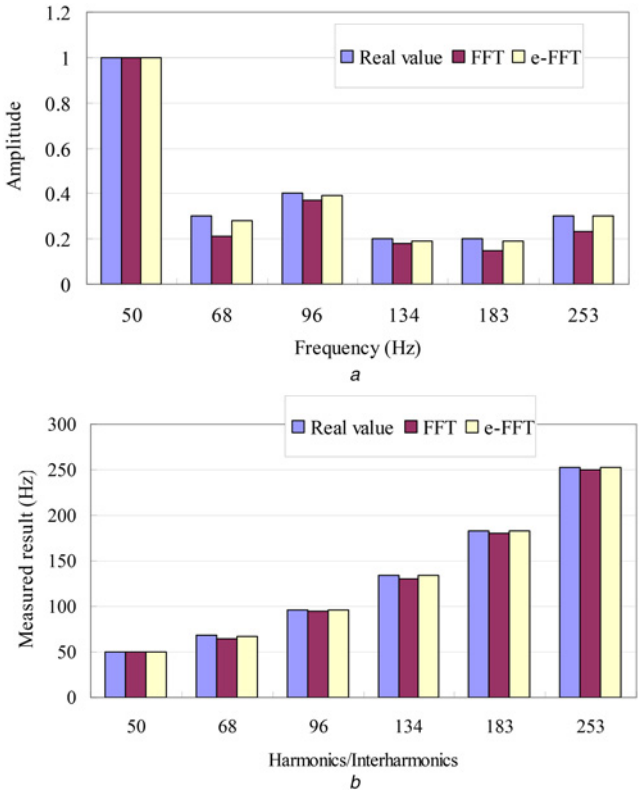

Fig. 6 *Comparisons of FFT and e-FFT with Δf = 5 Hz*
a Amplitude measurement
b Frequency measurement

3.1.2 Analysis with Δf = 2.5 Hz: The parameters of e-FFT model are set as $f_s = 1.28$ kHz, N = 512, i.e. $\Delta f = 2.5$ Hz. The interharmonics analysis using e-FFT model is carried out by the following five cases from (17). According to the rule of group bandwidth (τ) selection, τ is chosen as follows. The spectrum of $s(t)$ using FFT is shown in Fig. 7. It is obvious that a considerable dispersed power always comes with interharmonics and thus causes incorrect results.

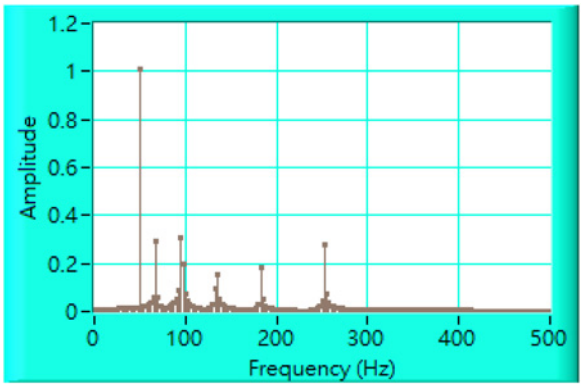

Fig. 7 *Spectrum of s(t) using FFT with Δf = 2.5 Hz*

(i) For $f_{i1} = 68$ Hz, $6\Delta f(=15) \le |f_{i1} - f_1| = |68 - 50| < 8\Delta f(=20) \Rightarrow \tau = 3$
(ii) For $f_{i2} = 96$ Hz, $|f_{i2} - f_{i1}| = |96 - 68| \ge 10\Delta f(=25) \Rightarrow \tau = 5$
(iii) For $f_{i3} = 134$ Hz, $|f_{i3} - f_{i2}| = |134 - 96| \ge 10\Delta f(=25) \Rightarrow \tau = 5$
(iv) For $f_{i4} = 183$ Hz, $|f_{i4} - f_{i3}| = |183 - 134| \ge 10\Delta f(=25) \Rightarrow \tau = 5$
(v) For $f_{i5} = 253$ Hz, $|f_{i5} - f_{i4}|(=253 - 183) \ge 10\Delta f(=25) \Rightarrow \tau = 5$

Case 1: $a_{i1} = 0.3, f_{i1} = 68$ Hz, $\tau = 3$

$$\Delta f_k = \frac{\sqrt{0.06^2 + 0.022^2 + 0.015^2}}{\sqrt{0.036^2 + 0.057^2 + 0.29^2 + \sqrt{0.06^2 + 0.022^2 + 0.015^2}}} \cdot \Delta f = \frac{0.07}{0.3 + 0.07} \cdot 2.5 \simeq 0.47\,(\text{Hz}) \tag{28}$$

$$\text{R.A.} = \sqrt{0.036^2 + 0.057^2 + 0.29^2 + 0.06^2 + 0.022^2 + 0.015^2} \simeq 0.3 \tag{29}$$

The measured frequency is equal to $f_k = 67.5$ Hz plus $\Delta f_k = 0.47$ Hz, i.e. 67.97 Hz, almost same as the real one (68 Hz). On the other hand, the measured amplitude is ~0.3 that is also same as the real one (0.3).

Case 2: $a_{i2} = 0.4, f_{i2} = 96$ Hz, $\tau = 5$

(see equations (30) and (31))

The measured frequency is equal to $f_k = 95$ Hz plus $\Delta f_k = 1.0$ Hz, i.e. 96 Hz, same as the real one (96 Hz). The measured amplitude is ~0.39 that is very close to the real one (0.4).

Case 3: $a_{i3} = 0.2, f_{i3} = 134$ Hz, $\tau = 5$

(see equations (32) and (33))

The measured frequency is equal to $f_k = 132.5$ Hz plus $\Delta f_k = 1.57$ Hz, i.e. 134.07 Hz, almost same as the real one (134 Hz).

$$\Delta f_k = \frac{\sqrt{0.2^2 + 0.074^2 + 0.044^2 + 0.031^2 + 0.023^2}}{\sqrt{0.027^2 + 0.035^2 + 0.051^2 + 0.087^2 + 0.3^2 + \sqrt{0.2^2 + 0.074^2 + 0.044^2 + 0.031^2 + 0.023^2}}} \cdot \Delta f = \frac{0.22}{0.32 + 0.22} \cdot 2.5 \simeq 1.0\,(\text{Hz}) \tag{30}$$

The measured amplitude is ∼0.196 that is very close to the real one (0.2).

Case 4: $a_{i4} = 0.2, f_{i4} = 183$ Hz, $\tau = 5$

(see equations (34) and (35))

The above results indicate that the measured frequency is equal to $f_k = 182.5$ Hz plus $\Delta f_k = 0.6$ Hz, i.e. 183.1 Hz, almost same as the real one (183 Hz). The measured amplitude is ∼0.196 that is very close to the real one (0.2).

Case 5: $a_{i5} = 0.3, f_{i5} = 253$ Hz, $\tau = 5$

(see equations (36) and (37))

As above, the measured frequency is equal to $f_k = 252.5$ Hz plus $\Delta f_k = 0.6$ Hz, i.e. 253.1 Hz, almost same as the real one (253 Hz). The measured amplitude is ∼0.29 that is very close to the real one (0.3).

The measured spectrum using e-FFT is shown in Fig. 8, revealing no dispersed power around harmonics/interharmonics.

The comparison between FFT and e-FFT is concluded in Fig. 9. It can be seen that the results from e-FFT model with $\Delta f = 2.5$ Hz provides even better performance outcomes than $\Delta f = 5$ Hz. Although the measurement in frequency estimation is improved from traditional FFT, it cannot achieve a correct analysis for most of amplitude estimation. The maximum error for amplitude and frequency estimation using FFT is 20 and 1.12%, respectively. On the other hand, the maximum error for amplitude and frequency estimation using e-FFT is only 3.33 and 0.05%, respectively.

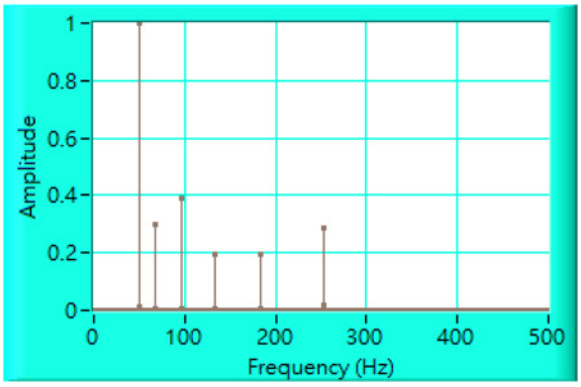

Fig. 8 *Spectrum of s(t) using e-FFT with Δf = 2.5 Hz*

3.1.3 Analysis with Δf = 10 Hz: The parameters of e-FFT model are set as $f_s = 1.28$ kHz, $N = 128$, i.e. $\Delta f = 10$ Hz. The interharmonics analysis using e-FFT model is carried out by the following five cases from (17). According to the rule of group bandwidth (τ) selection, τ is chosen as follows. The spectrum of $s(t)$ using FFT with $\Delta f = 10$ Hz is shown in Fig. 10.

(i) For $f_{i1} = 68$ Hz, $|f_{i1} - f_1| = |68 - 50| < 4\Delta f (= 40) \Rightarrow \tau = 1$

$$\text{R.A.} = \sqrt{0.027^2 + 0.035^2 + 0.051^2 + 0.087^2 + 0.3^2 + 0.2^2 + 0.074^2 + 0.044^2 + 0.031^2 + 0.023} \simeq 0.39 \tag{31}$$

$$\Delta f_k = \frac{\sqrt{0.16^2 + 0.048^2 + 0.03^2 + 0.022^2 + 0.018^2}}{\sqrt{0.00008^2 + 0.00014^2 + 0.00031^2 + 0.001^2 + 0.0091^2} + \sqrt{0.16^2 + 0.048^2 + 0.03^2 + 0.022^2 + 0.018^2}} \cdot \Delta f = \frac{0.17}{0.1 + 0.17} \cdot 2.5 \simeq 1.57\,(\text{Hz}) \tag{32}$$

$$\text{R.A.} = \sqrt{0.00008^2 + 0.00014^2 + 0.00031^2 + 0.001^2 + 0.0091^2 + 0.16^2 + 0.048^2 + 0.03^2 + 0.022^2 + 0.018^2} \simeq 0.196 \tag{33}$$

$$\Delta f_k = \frac{\sqrt{0.05^2 + 0.024^2 + 0.017^2 + 0.013^2 + 0.011^2}}{\sqrt{0.0069^2 + 0.0089^2 + 0.014^2 + 0.028^2 + 0.18^2} + \sqrt{0.05^2 + 0.024^2 + 0.017^2 + 0.013^2 + 0.011^2}} \cdot \Delta f = \frac{0.06}{0.187 + 0.06} \cdot 2.5 \simeq 0.6\,(\text{Hz}) \tag{34}$$

$$\text{R.A.} = \sqrt{0.0069^2 + 0.0089^2 + 0.014^2 + 0.028^2 + 0.18^2 + 0.05^2 + 0.024^2 + 0.017^2 + 0.013^2 + 0.011^2} \simeq 0.196 \tag{35}$$

$$\Delta f_k = \frac{\sqrt{0.075^2 + 0.036^2 + 0.025^2 + 0.019^2 + 0.016^2}}{\sqrt{0.0086^2 + 0.013^2 + 0.021^2 + 0.042^2 + 0.28^2} + \sqrt{0.075^2 + 0.036^2 + 0.025^2 + 0.019^2 + 0.016^2}} \cdot \Delta f = \frac{0.09}{0.28 + 0.09} \cdot 2.5 \simeq 0.6\,(\text{Hz}) \tag{36}$$

$$\text{R.A.} = \sqrt{0.0086^2 + 0.013^2 + 0.021^2 + 0.042^2 + 0.28^2 + 0.075^2 + 0.036^2 + 0.025^2 + 0.019^2 + 0.016^2} \simeq 0.29 \tag{37}$$

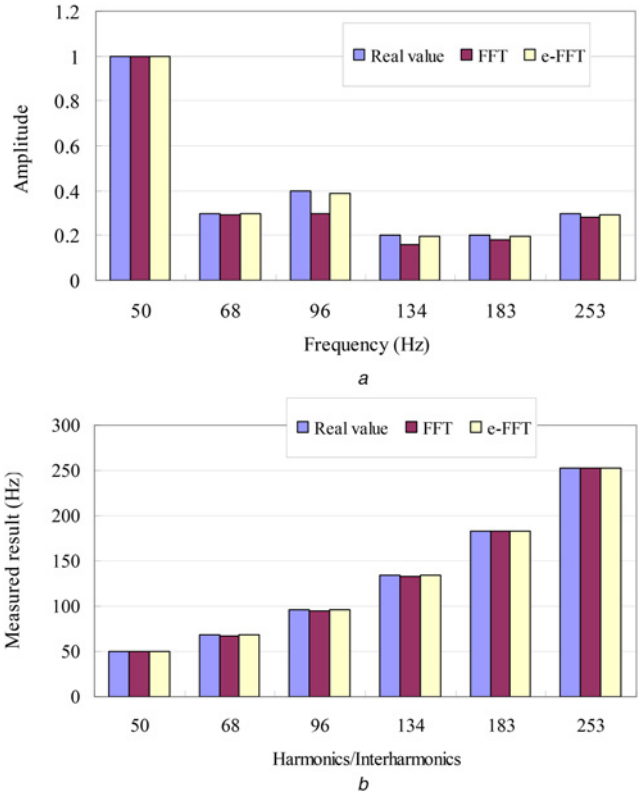

Fig. 9 *Comparisons of FFT and e-FFT with Δf = 2.5 Hz*
a Amplitude measurement
b Frequency measurement

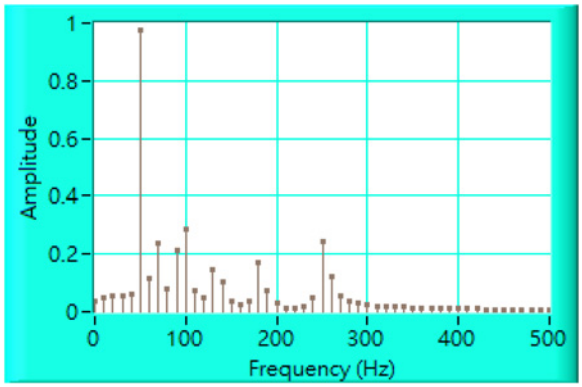

Fig. 10 *Spectrum of s(t) using FFT with Δf = 10 Hz*

(ii) For $f_{i2} = 96$ Hz, $|f_{i2} - f_{i1}| = |96 - 68| < 4\Delta f(=40) \Rightarrow \tau = 1$
(iii) For $f_{i3} = 134$ Hz, $|f_{i3} - f_{i2}| = |134 - 96| < 4\Delta f(=40) \Rightarrow \tau = 1$
(iv) For $f_{i4} = 183$ Hz, $4\Delta f(=40) \le |f_{i4} - f_{i3}| = |183 - 134| < 6\Delta f(=60) \Rightarrow \tau = 2$
(v) For $f_{i5} = 253$ Hz, $6\Delta f(=60) \le |f_{i5} - f_{i4}|(=253 - 183) < 8\Delta f(=80) \Rightarrow \tau = 3$

Case 1: $a_{i1} = 0.3, f_{i1} = 68$ Hz, $\tau = 1$

$$\Delta f_k = \frac{\sqrt{0.24^2}}{\sqrt{0.076^2 + 0.12^2} + \sqrt{0.24^2}} \cdot \Delta f = \frac{0.24}{0.14 + 0.24} \cdot 10 \simeq 6.32\,(\text{Hz}) \tag{38}$$

$$\text{R.A.} = \sqrt{0.076^2 + 0.12^2 + 0.24^2} \simeq 0.28 \tag{39}$$

The measured frequency is equal to $f_k = 60$ Hz plus $\Delta f_k = 6.3$ Hz, i.e. 66.3 Hz, close to the real one (68 Hz). On the other hand, the measured amplitude is ~0.28 that is also close to the real one (0.3).

Case 2: $a_{i2} = 0.4, f_{i2} = 96$ Hz, $\tau = 1$

$$\Delta f_k = \frac{\sqrt{0.29^2}}{\sqrt{0.079^2 + 0.21^2} + \sqrt{0.29^2}} \cdot \Delta f = \frac{0.29}{0.23 + 0.29} \cdot 10 \simeq 5.6\,(\text{Hz}) \tag{40}$$

$$\text{R.A.} = \sqrt{0.079^2 + 0.21^2 + 0.29^2} \simeq 0.37 \tag{41}$$

The measured frequency is equal to $f_k = 90$ Hz plus $\Delta f_k = 5.6$ Hz, i.e. 95.6 Hz, very close to the real one (96 Hz). The measured amplitude is ~0.37 that is close to the real one (0.4).

Case 3: $a_{i3} = 0.2, f_{i3} = 134$ Hz, $\tau = 1$

$$\Delta f_k = \frac{\sqrt{0.1^2}}{\sqrt{0.048^2 + 0.15^2} + \sqrt{0.1^2}} \cdot \Delta f = \frac{0.1}{0.16 + 0.1} \cdot 10 \simeq 3.8\,(\text{Hz}) \tag{42}$$

$$\text{R.A.} = \sqrt{0.048^2 + 0.15^2 + 0.1^2} \simeq 0.19 \tag{43}$$

The measured frequency is equal to $f_k = 130$ Hz plus $\Delta f_k = 3.8$ Hz, i.e. 133.8 Hz, almost same as the real one (134 Hz). The measured amplitude is ~0.19 that is very close to the real one (0.2).

Case 4: $a_{i4} = 0.2, f_{i4} = 183$ Hz, $\tau = 2$

$$\Delta f_k = \frac{\sqrt{0.074^2 + 0.029^2}}{\sqrt{0.036^2 + 0.17^2} + \sqrt{0.074^2 + 0.029^2}} \cdot \Delta f = \frac{0.08}{0.17 + 0.08} \cdot 10 \simeq 3.2\,(\text{Hz}) \tag{44}$$

$$\text{R.A.} = \sqrt{0.036^2 + 0.17^2 + 0.074^2 + 0.029^2} \simeq 0.19 \tag{45}$$

The measured frequency is equal to $f_k = 180$ Hz plus $\Delta f_k = 3.2$ Hz, i.e. 183.2 Hz, very close to the real one (183 Hz). The measured amplitude is ~0.19 that is very close to the real one (0.2).

Case 5: $a_{i5} = 0.3, f_{i5} = 253$ Hz, $\tau = 3$

$$\Delta f_k = \frac{\sqrt{0.12^2 + 0.056^2 + 0.038^2}}{\sqrt{0.019^2 + 0.046^2 + 0.25^2} + \sqrt{0.12^2 + 0.056^2 + 0.038^2}} \cdot \Delta f = \frac{0.14}{0.255 + 0.14} \cdot 10 \simeq 3.5\,(\text{Hz}) \tag{46}$$

$$\text{R.A.} = \sqrt{0.019^2 + 0.046^2 + 0.25^2 + 0.12^2 + 0.056^2 + 0.038^2} \simeq 0.29 \tag{47}$$

As above, the measured frequency is equal to $f_k = 250$ Hz plus $\Delta f_k = 3.5$ Hz, i.e. 253.5 Hz, very close to the real one (253 Hz). The measured amplitude is ~0.29 that is very close to the real one (0.3).

The measured spectrum using e-FFT is shown in Fig. 11, indicating no dispersed power around harmonics/interharmonics.

The comparison between FFT and e-FFT is concluded in Fig. 12. Clearly, the results from e-FFT model are close to the real values for either amplitude or frequency identification, but traditional FFT is unable to achieve a correct analysis except at fundamental

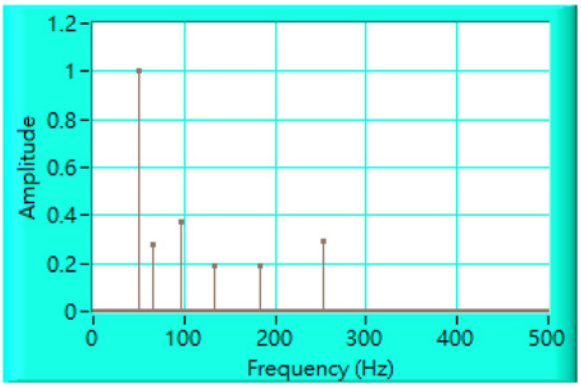

Fig. 11 *Spectrum of s(t) using e-FFT with Δf = 10 Hz*

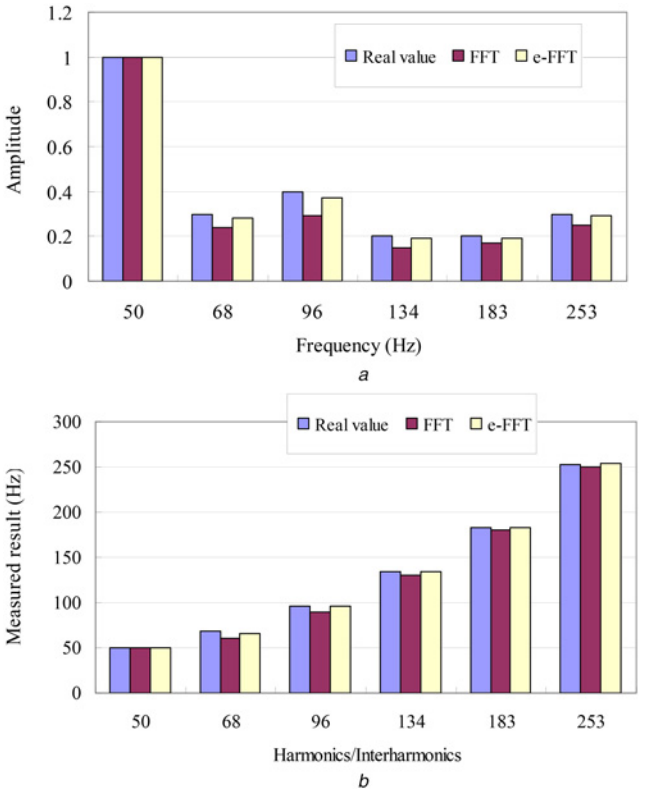

Fig. 12 *Comparisons of FFT and e-FFT with Δf = 10 Hz*
a Amplitude measurement
b Frequency measurement

component (50 Hz). The maximum error for amplitude and frequency estimation using FFT is up to 27.5 and 11.76%, respectively. By contrast, the maximum error for amplitude and frequency estimation using e-FFT is only 7.5 and 2.5%, respectively.

3.2 Determination of group bandwidth (τ), sampled point (N) and sampling rate (f_s)

The group bandwidth (τ) may influence the measurement accuracy, and it should be chosen appropriately. The larger group bandwidth (τ) can collect all dispersed power and then regain the actual amplitude more accurately. However, a large τ may lead to a dispersed power overlapping within near major harmonics. For this reason, τ should be chosen sufficiently large but to avoid the overlapping from neighbour harmonics. The selection rule of τ (1–5) is thus formulated depending on the distribution range of dispersed energy.

It notes that the N is chosen as $N = 2^m$, e.g. 64, 128, 256, 512, 1024,….., using $f_s = 1.28$ kHz, where $\Delta f = 20, 10, 5, 2.5, 1.25, ...$, respectively. Correspondingly, the sampling time will take 50, 100, 200, 400, 800 ms etc., respectively. Clearly, an increasing N can obtain lower Δf, but it will sacrifice for longer sampling time. Hence, a compromise should be reached by both Δf and sampling time.

4 Conclusions

Although FFT is now widely applied to harmonics analysis, it cannot be directly delivered to interharmonics measurement. From the proposed e-FFT model, the dispersed energy can be collected efficiently and the interharmonic original amplitude is thus retrieved. In addition, the interharmonic frequency can be found using a simple arithmetic computation. The selection of group bandwidth (τ) has been formulated to effectively avoid overlapping between two close interharmonics. In this model, $\Delta f = 5$ Hz is chosen based on a compromise between the measurement accuracy and sampling time. Accordingly, even a rapid change of signal variation can be responded sufficiently fast. For future work, it is suggested to study the case that is involved in different harmonics sources. This situation may generate unexpected sideband interharmonic frequencies that cannot be resolved by current techniques.

5 References

[1] Testa A., Akram M.F., Burch R., *ET AL.*: 'Interharmonics: theory and modeling', *IEEE Trans. Deliv.*, 2007, **22**, (4), pp. 2335–2348
[2] Karimi-Ghartemani M., Reza Iravani M.: 'Measurement of harmonics/inter-harmonics of time-varying frequency', *IEEE Trans. Power Deliv.*, 2005, **20**, (1), pp. 23–31
[3] Lin H.C.: 'Identification of interharmonics using disperse energy distribution algorithm for flicker troubleshooting', *IET Sci. Meas. Technol.*, 2016, **10**, (7), pp. 786–794
[4] Tayjasanant T., Wang W., Li C., *ET AL.*: 'Interharmonic-flicker curves', *IEEE Trans. Power Deliv.*, 2005, **20**, (2), pp. 1017–1024
[5] Li C., Xu W., Tayjasanant T.: 'Interharmonics: basic concepts and techniques for their detection and measurement', *Electr. Power Syst. Res.*, 2003, **66**, (1), pp. 39–48
[6] Lin H.C.: 'Separation of adjacent interharmonics using maximum energy retrieving algorithm', *IET Sci. Meas. Technol.*, 2016, **10**, (2), pp. 92–99
[7] Lin H.C.: 'Fast tracking of time-varying power system frequency and harmonics using iterative-loop approaching algorithm', *IEEE Trans. Ind. Electron.*, 2007, **54**, (2), pp. 974–983
[8] Aghazadeh R., Lesani H., Sanaye-Pasand M., *ET AL.*: 'New technique for frequency and amplitude estimation of power system signals', *IEE Gener. Transm. Distrib.*, 2005, **152**, (3), pp. 435–440
[9] Lobos T., Kozina T., Koglin H.-J.: 'Power system harmonics estimation using linear least squares method and SVD', *IEE Proc., IEE Gener. Transm. Distrib.*, 2001, **148**, (6), pp. 567–572
[10] Zhu T.X.: 'Exact harmonics/interharmonics calculation using adaptive window width', *IEEE Trans. Power Deliv.*, 2007, **22**, (4), pp. 2279–2288
[11] Chang G.W., Chen C.-I.: 'An accurate time-domain procedure for harmonics and interharmonics detection', *IEEE Trans. Power Deliv.*, 2010, **25**, (3), pp. 1787–1795
[12] Jain S.K., Singh S.N.: 'Exact model order ESPRIT technique for harmonics and interharmonics estimation', *IEEE Trans. Instrum. Meas.*, 2012, **61**, (7), pp. 1915–1923
[13] Wu R.-C., Tai C.C.: 'Analysis of the exponential signal by the interpolated DFT algorithm', *IEEE Trans. Instrum. Meas.*, 2010, **59**, (12), pp. 3306–3317
[14] Gu I.Y.H., Bollen M.H.J.: 'Estimating interharmonics by using sliding-window ESPRIT', *IEEE Trans. Power Deliv.*, 2008, **23**, (1), pp. 13–23
[15] He C., Shu Q.: 'Separation and analyzing of harmonics and interharmonics based on single channel independent component analysis', *Int. Trans. Electr. Energy Syst.*, 2015, **25**, pp. 169–179
[16] Lin H.C., Chen C.H., Liu L.Y.: 'Harmonics and Interharmonics Measurement using Group-harmonic Power Minimizing Algorithm'. Proc. of the World Congress on Engineering, London, U.K., July 2011, pp. 1300–1305

[17] Lin H.C.: 'Intelligent neural network based adaptive power line conditioner for real-time harmonics filtering', *IEE Proc., IEE Gener. Transm. Distrib.*, 2004, **151**, (5), pp. 561–567
[18] Chen C.I.: 'Virtual multifunction power quality analyzer based on adaptive linear neural network', *IEEE Trans. Ind. Electron.*, 2012, **59**, (8), pp. 3321–3329
[19] Valtierra-Rodriguez M., de Jesus Romero-Troncoso R., Osornio-Rios R.A., *ET AL.*: 'Detection and classification of single and combined power quality disturbances using neural networks', *IEEE Trans. Ind. Electron.*, 2014, **61**, (5), pp. 2473–2482
[20] IEC 61000-4-7: Electromagnetic compatibility (EMC) Part 4: testing and measurement techniques Section 7: general guide on harmonics and interharmonics measurements and instrumentation for power supply systems and equipment connected thereto, 2002
[21] Oppenheim A.V., Schafer R.W.: 'Discrete-time signal processing' (Prentice Hall, Upper Saddle River, NJ, 1989)
[22] Press W.H., Flannery B.P., Teukolsky S.A., *ET AL.*: 'Numerical recipes-The art of scientific computing' (Cambridge University Press, Cambridge, 1986)
[23] Lin H.C.: 'Development of leakage energy allocation approach for time-varying interharmonics tracking', *IET Gener. Transm. Distrib.*, 2015, **9**, (9), pp. 798–804
[24] Lin H.C., Ye Y.C., Huang B.J., *ET AL.*: 'Bearing vibration detection and analysis using enhanced fast Fourier transform algorithm', *Adv. Mech. Eng.*, 2016, **8**, (10), pp. 1–14